

Comparative Molecular Field Analysis of Caspase-3 Inhibitors

Sathya. B and Thirumurthy Madhavan[†]

Abstract

Caspases, a family of cysteinyl aspartate-specific proteases plays a central role in the regulation and the execution of apoptotic cell death. Activation of caspases-3 stimulates a signaling pathway that ultimately leads to the death of the cell. Hence, caspase-3 has been proven to be an effective target for reducing the amount of cellular and tissue damage. In this work, comparative molecular field analysis (CoMFA) was performed on a series of 3, 4-dihydropyrimidindolones derivatives which are inhibitors of caspase-3. The best predictions were obtained for CoMFA model ($q^2=0.676$, $r^2=0.990$). The predictive ability of test set (r^2_{pred}) was 0.688. Statistical parameters from the generated QSAR models indicated the data is well fitted and have high predictive ability. Our theoretical results could be useful to design novel and more potent caspase-3 derivatives.

Key words: Caspase-3, CoMFA

1. Introduction

Caspases, a family of cysteinyl aspartate-specific proteases which mediates the signaling pathway and plays a central role in the regulation and the execution of apoptotic cell death^[1-4]. Caspases are synthesized as zymogens (pro-caspase) which are activated by various triggers and cause the active caspase to express itself and carry out specific function. It cleaves target proteins at specific aspartate residues^[5]. Caspases are essential effector molecules for carrying out apoptosis in eukaryotic cells^[4]. The apoptotic caspases are classified as initiators or executioners, depending on their point of entry into the apoptotic cascade. Till now 11 known human caspases has been discovered and which can be divided into three sub-types based on their structure and function^[3]. Group I caspases (1, 4, 5 and 14) are primarily involved in inflammation. Group II caspases (6, 8, 9 and 10) are primary involved in apoptosis as upstream regulators of the Group III caspases (3 and 7). The Group III caspases are effector caspases that, once activated, stimulate a signaling pathway that ultimately leads to the death of the cell^[6]. Failure of apoptosis is one of the

main contributions to tumour development and autoimmune diseases; this coupled with unwanted apoptosis that occurs with ischemia or Alzheimer's disease, has stimulated interest in caspases as potential therapeutic targets for drug development^[7].

Recent study has shown that caspase inhibition can help in tissue protection^[8-12]. The basic structural feature of almost all known caspase inhibitors is an electrophilic group that lead to inactivation of the enzyme by forming reversible or irreversible bond with the active site cysteine^[13]. Caspases-3 is common to all currently known caspases^[6,14] and plays a key role in apoptosis among several different groups of caspase enzymes^[15]. Many groups have been reported their efforts toward selective, small molecule caspase-3 inhibitors^[16-19]. Caspase-3 has been proven to be an effective target for reducing the amount of cellular and tissue damage in cell culture and animal models by specific inhibitors^[11,20]. Till to date, many studies have been published in which the combination of 2D and 3D-QSAR techniques have proven the successful role in the modern drug discovery process^[21]. We formulate a reasonable 3D-QSAR model based on ligand alignment. Our study thoroughly discussed the CoMFA models for a set of caspase-3 inhibitors and emphasized the significant parameters for higher activity. Our optimum QSAR models could be a good starting point for ligand optimization and guidance for medicinal chemist to

¹Department of Bioinformatics, School of Bioengineering, SRM University, SRM Nagar, Kattankulathur, Chennai 603203, India

[†]Corresponding author : thiru.murthyunom@gmail.com
(Received : September 12, 2014, Revised : September 23, 2014, Accepted : September 25, 2014)

derive future non-peptidic inhibitors of caspase-3 derivatives.

2. Experimental Section

2.1. Dataset

A series 35 compounds has been taken from the literature with their biological activities in terms of IC_{50} values^[19]. These are identified as lead series of novel 3,4-dihydropyrimidindolones and considered as potent and selective inhibitors of caspase-3. The binding affin-

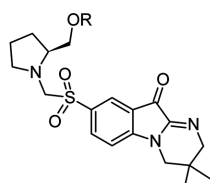
ities of given pyrimidindolones concentration in nano molar (nM) range were converted to the molar (M) concentration and then converted to logarithmic scale for further QSAR analyses on dataset, using the following formula.

$$pIC_{50} = -\log (IC_{50})$$

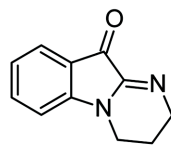
Total dataset is divided randomly into a training set of 27 compounds and test set (wide range of activity) of 8 compounds which has been shown in Table 1.

Table 1. Structures and biological activities (pIC_{50}) of caspase-3 inhibitors

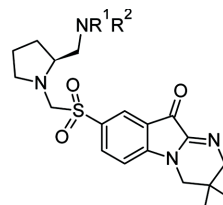
Compound	R	NR ¹ R ²	n	pIC_{50}
1	Phenyl	-	-	8.155
2	4-F-phenyl	-	-	7.968
3	4-OCH ₃ -phenyl	-	-	7.859
4*	4-Cl phenyl	-	-	7.432
5	4-Ac phenyl	-	-	7.523
6*	4-t-Bu phenyl	-	-	7.092
7	4-F-3-CH ₃ phenyl	-	-	7.638
8	4-OCH ₃ -2-Cl phenyl	-	-	7.086
9	2-Pyridyl	-	-	8.107
10*	5-Cl 2-pyridyl	-	-	7.990
11	6-CH ₃ 2-pyridyl	-	-	7.901



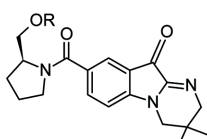
Compound 1-15



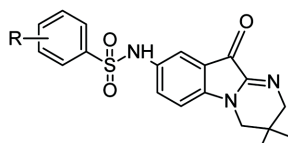
General Structure



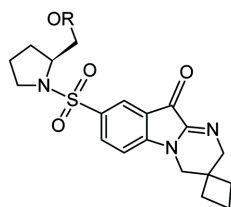
Compound 16-19



Compound 20-21

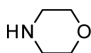
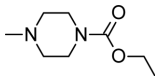
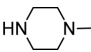
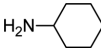


Compound 22-29



Compound 30-35

Table 1. Continued

Compound	R	NR ¹ R ²	n	pIC ₅₀
12	3-pyridyl	-	-	8.620
13	5-Cl 3-pyridyl	-	-	8.354
14*	2-CH ₃ 3-pyridyl	-	-	8.144
15	5-CO ₂ CH ₃ 3-pyridyl	-	-	7.994
16	-		-	8.302
17	-		-	7.844
18*	-		-	7.360
19	-		-	7.229
20*	Ph	-	-	4.301
21	CH ₃	-	-	6.000
22	H	-	-	6.439
23*	2-F	-	-	6.830
24	3-CF ₃	-	-	6.719
25	3-OCH ₃	-	-	6.456
26	4-Cl	-	-	5.874
27	4-OCH ₃	-	-	5.823
28*	4-OCF ₃	-	-	5.598
29	4-F	-	-	5.621
30	CH ₃	-	1	8.481
31	Ph	-	1	8.889
32	CH ₃	-	2	7.829
33	Ph	-	2	8.365
34	CH ₃	-	3	7.866
35	Ph	-	3	7.609

*Test set compounds

2.2. Molecular Modeling

All computational studies were performed using molecular modeling package SYBYL 8.1 installed on a Linux system. The initial step is to find out the most active molecule within the dataset. Random search method has been done to derive the least energy conformation which is considered as a bioactive conformation and it is then minimized by applying Tripos force field. Finally Gasteiger-Hückel charges were applied to all the molecules of dataset and it was subsequently used for QSAR studies. As compound 31 was the most active, all the possible conformations were obtained by systematic conformational analysis and the lowest energy conformer was assumed as bioactive conformer

and was chosen for subsequent QSAR modeling. Using this particular conformer structure as standard, bioactive conformations for other compounds were determined by systematic conformer search for the additional moieties, by keeping core part constrained. In this way, the common scaffold of every inhibitor occupies the same area in three-dimensional space.

2.3. Alignment Method

The accuracy and reliability of the CoMFA is directly dependent on the structural alignment rule^[22]. The quality of ligand alignment plays very essential role. Conformational energies were computed with electrostatic term, and the lowest energy conformer was

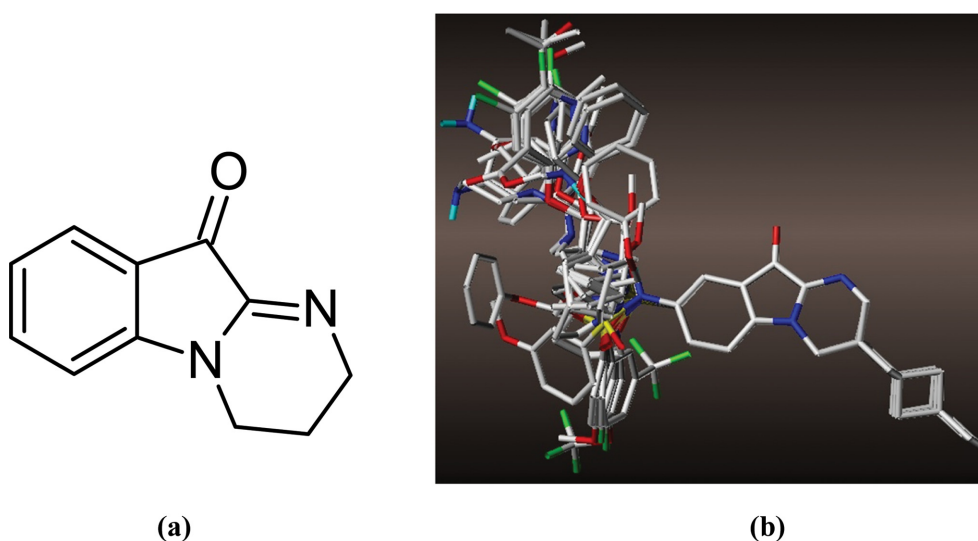


Fig. 1. (a) Maximum common substructure for atom by atom matching. (b) Superimposed structures after optimization with Gasteiger-Hückel charge.

selected as template molecule. The most active molecule was used as the reference to align all the compounds using atom-to-atom matching. The minimized structures were aligned over the template using the atom fit option in Sybyl, and subsequently, this alignment was used for CoMFA analysis. The matching atoms were selected by maximum common substructure (MCS) as shown in Fig. 1(a) and the alignment of the all the molecules are represented in Fig. 1(b).

2.4. CoMFA Model Generation

CoMFA calculations were carried out by applying the default settings in Sybyl 8.1. For the alignment set, the steric and electrostatic CoMFA field was calculated at each lattice intersection of a regularly spaced grid of 2.0 unit. The standard CoMFA field performed the Lennard-Jones potential and the Coulombic potential, for the steric and electrostatic fields, respectively. The Van der Waals potential and columbic terms, which represent steric and electrostatic fields, respectively, were calculated using Tripos force field. A distance-dependent dielectric constant was used. A sp^3 carbon atom with a Van der Waals radius of 1.52 Å and a charge of +1.0 served as the probe atom to calculate steric and electrostatic fields. The steric and electrostatic contributions were truncated to ± 30 kcal/mol, and

electrostatic contributions were ignored at lattice intersections with maximum steric interactions. With standard option for the scaling of variables, the regression analysis was carried out using cross-validated partial least squares approach (PLS) of LOO (leave-one-out)^[23]. After the optimal number of components was determined, a non-cross-validated analysis was carried out without column filtering.

2.5. Partial Least Squares (PLS) Analysis

In 3D-QSAR, the CoMFA descriptors were used as independent variables and pIC_{50} values were used as the dependent variable. The PLS method was used to linearly correlate these CoMFA descriptors with the biological activity values. The CoMFA cutoff values were set to 30 kcal/mol for both the steric and electrostatic fields, and all fields were scaled by the default options in SYBYL. Cross-validation analysis was performed using the LOO method. The cross-validated correlation coefficient (q^2) that resulted in optimum number of components and lowest standard error of prediction were considered for further analysis.

3. Results and Discussion

In the present work, we have applied CoMFA on a set of non-peptidic inhibitors derivatives to build 3D-

QSAR models. During model generation, we have formulated different strategies in order to derive statistically robust QSAR model. The best predictions were obtained for CoMFA model ($q^2=0.676$, $r^2=0.990$). Finally, the obtained value was used for further analysis in order to generate CoMFA steric and electrostatic contour plots.

3.1. CoMFA Model Analysis

The optimum CoMFA model was derived with the combination of steric and electrostatic field contribution and Gasteiger-Hückel charge method with 2.0 Å grid space. The Leave one out (LOO) analysis gave the cross-validated q^2 of 0.676 with six components and non cross-validated PLS analysis resulted in a correlation coefficient r^2 of 0.990, $F=340.166$, and an estimated standard error of 0.103. Statistical results obtained from the constructed model verified the predictive ability of the model (Table 2) and further implied that the steric and electrostatic factors contribute to the binding affinities. The predictive ability of the developed CoMFA model was assessed by the test set (five molecules) predictions, which were excluded during CoMFA model generation. The predictive ability of the test set was 0.688. CoMFA contour maps for steric field with highly active compound 31, where green contour indicates regions where bulky groups increases activity and yellow contours indicates bulky groups decreases activity (Fig. 2). CoMFA contour maps for electrostatic field with highly active compound 31,

where blue contour indicates regions where electropositive groups increases activity and red contours indicates regions where electronegative groups increases activity (Fig. 3).

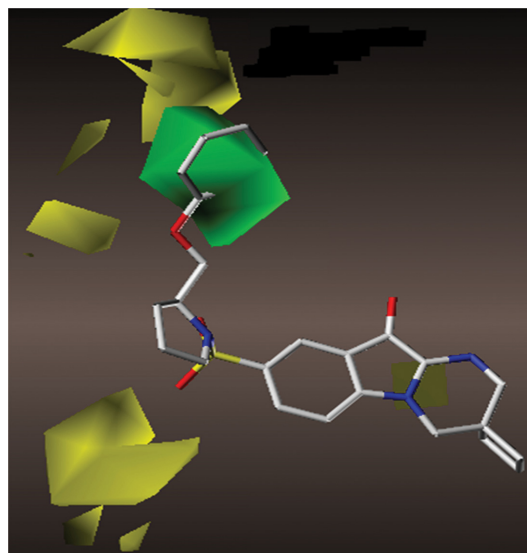


Fig. 2. CoMFA contour maps for steric field with highly active compound 31, where green contour indicates regions where bulky groups increases activity and yellow contours indicates bulky groups decreases activity.

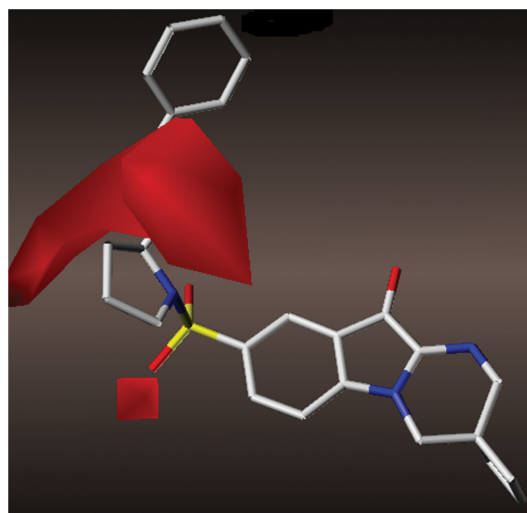


Fig. 3. CoMFA contour maps for electrostatic field with highly active compound 31, where blue contour indicates regions where electropositive groups increases activity and red contours indicates regions where electronegative groups increases activity.

Table 2. Statistical results of CoMFA models

PLS statistics	CoMFA model Ligand-based alignment
q^2	0.676
N	6
r^2	0.990
SEE	0.103
F-value	340.166
r^2_{pred}	0.688
Field contribution	
Steric	0.867
Electrostatic	0.133

q^2 = cross-validated correlation coefficient; N= number of statistical components; r^2 = non-cross validated correlation coefficient; SEE=standard estimated error; F=Fisher value; $r^2_{predictive}$ = predictive correlation coefficient for test set.

4. Conclusions

In the present study, we developed satisfactory 3D-QSAR models of non-peptidic derivatives using CoMFA based on the atom-by-atom matching alignment. We have been formulated different strategies in order to derive statistically robust 3D-QSAR models. The 3D-QSAR results revealed some important sites, where steric, electrostatic, hydrophobic modifications could significantly affect the bioactivities of the compounds. The information's have gathered from CoMFA studies demonstrated the way to understand the structural and chemical features of non-peptidic derivatives in designing and finding new potential caspase-3 inhibitors.

References

- [1] M. D. Jacobson, M. Weil, and M. C. Raff, "Programmed cell death in animal development", *Cell*, Vol. 88, pp. 347-54, 1997.
- [2] G. M. Cohen, "Caspases: the executioners of apoptosis", *J. Biochem.*, Vol. 326, pp. 1-16, 1997.
- [3] C. B. Thonberry and Y. Lazebnik, "Caspases: enemies within", *Science*, Vol. 281, pp. 1312-1316, 1998.
- [4] D. W. Nicholson, "Caspase structure, proteolytic substrates, and function during apoptotic cell death", *Cell Death Differ.*, Vol. 6, pp. 1028-1042, 1999.
- [5] J. Wang and M. J. Lenardo, "Roles of caspases in apoptosis, development and cytokine maturation revealed by homozygous gene deficiencies", *J. Cell Sci.*, Vol. 113, pp. 753-757, 2000.
- [6] R. E. Endres, S. Namura, M. Shomizu-Sasamata, C. Waeber, L. Zhang, T. Gomez-Isla, B. T. Hyman, and M. A. Moskowitz, "Attenuation of delayed neuronal death after mild focal ischemia in mice by inhibition of caspase family", *J. Cerebr. Blood F. Met.*, Vol. 18, pp. 238-247, 1998.
- [7] K. M. Boatright and G. S. Salvesen, "Mechanisms of caspase activation", *Curr. Opin. Cell Biol.*, Vol. 15, pp. 725-731, 2003.
- [8] B. A. Callus and D. L. Vaux, "Caspase inhibitors: viral, cellular and chemical", *Cell Death Differ.*, Vol. 14, pp. 73-78, 2007.
- [9] B. R. Hu, C. L. Liu, Y. Ouyang, K. Blomgren, and B. K. Siesjö, "Involvement of caspase-3 in cell death after hypoxia ischemia declines during brain maturation", *J. Cerebr. Blood F. Met.*, Vol. 20, pp. 1294-1300, 2000.
- [10] R. S. Hotchkiss, K. C. Chang, P. E. Swanson, K. W. Tinsley, J. J. Hui, P. Klender, S. Xanthoudakis, S. Roy, C. Black, E. Grimm, R. Aspiotis, Y. Han, D. W. Nicholson, and I. E. Karl, "Caspase inhibitors improves survival in sepsis: a critical role of the lymphocyte", *Nat. Immunol.*, Vol.1, pp. 496-501, 2000.
- [11] D. Lee, S. A. Long, J. H. Murray, J. L. Adams, M.E. Nuttall, D. P. Nadeau, K. Kikly, J. D. Winkler, C.-M. Sung, M. D. Ryan, M. A. Levy, P. M. Keller, and W. E. DeWolf, Jr, "Potent and selective non peptide inhibitors of caspase 3 and 7", *J. Med. Chem.*, Vol. 44, pp. 2015-2026, 2001.
- [12] H. Yaoita, K. Ogawa, K. Maehara, and Y. Maruyama, "Attenuation of ischemia/reperfusion injury in rats by a caspase inhibitor", *Circulation*, Vol. 97, pp. 276-281, 1998.
- [13] J. Schoenberger, J. Bauer, J. Moosbauer, C. Eilles, and D. Grimm, "Innovative strategies in in-vivo apoptosis imaging", *Curr. Med. Chem.*, Vol. 15, pp. 187-194, 2008.
- [14] D. K. Perry, M. J. Smyth, H. R. Stennicke, G. S. Salvesan, P. Duriez, G. G. Poirier, and Y. A. Hannun, "Zinc is a potent inhibitor of the apoptotic protease, caspase-3. A novel target for zinc in the inhibition of apoptosis", *J. Biol. Chem.*, Vol. 272, pp. 18530-18533, 1997.
- [15] G. Porter and R. U. Janicke, "Emerging roles of caspase 3 in apoptosis", *Cell Death Differ.*, Vol. 6, pp. 99-104, 1999.
- [16] C. W. Scott, C. Sobotka-Brinker, D. E. Wilkins, R. T. Jacobs, J. J. Folmer, W. J. Frazee, R. V. Bhat, S. V. Ghanekar, and D. Aharony, "Novel small molecule inhibitors of caspase-3 block cellular and biochemical features of apoptosis", *J. Pharmacol. Exp. Ther.*, Vol 304, pp. 433-440, 2003.
- [17] D. V. Kravchenko, V. M. Kysil, S. E. Tkachenko, S. Maliarchouk, I. M. Okun, and A. V. Ivanchtchenko, "Pyrrolo[3,4-c]quinoline-1,3-diones as potent caspase-3 inhibitors. Synthesis and SAR of 2-substituted 4-methyl-8-(morpholine-4-sulfonyl)-pyrrolo [3,4-c]quinoline-1,3-diones", *Eur. J. Med. Chem.*, Vol. 40, pp. 1377-1383, 2005.
- [18] W. Chu, J. Zhang, C. Zeng, J. Rothfuss, Z. Tu, Y. Chu, D.E. Reichert, M. J. Welch, and R. H. Mach, "N-Benzylisatin sulfonamide analogues as potent caspase-3 inhibitors: Synthesis, *in vitro* activity and molecular modeling studies", *J. Med. Chem.*, Vol. 48, pp. 7637-7647, 2005.
- [19] L. M. Havrana, D. C. Chonga, W. E. Childersa, P. J. Dollingsa, A. Dietricha, B. L. Harrisona, V. Mar-

- athiasa, G. Tawaa, A. Aulabaughb, R. Cowlingb, B. Kapoorb, W. Xuc, L. Mosyackc, F. Moyc, W.-T. Humc, A. Woodd, and A. J. Robichauda, "3,4-Dihydropyrimido(1,2-*a*)indol-10(2H) – ones as potent non-peptidic inhibitors of caspase-3", *Bioorgan. Med. Chem.*, Vol. 17, pp. 7755-7768, 2009.
- [20] R. S. Hotchkiss, K. C. Chang, P. E. Swanson, K. W. Tinsley, J. J. Hui, P. Klender, S. Xanthoudakis, S. Roy, C. Black, E. Grimm, R. Aspiotis, Y. Han, D. W. Nicholson, and I. E. Karl, "Caspase inhibitors improve survival in sepsis: a critical role of the lymphocyte", *Nat. Immunol.* Vol.1, pp. 496-501, 2000.
- [21] M. Thirumurthy, K. Gagan, G. Changdev, and S. J. Cho, "QSAR analysis on PfPK7 inhibitors using HQSAR, CoMFA and CoMSIA", *Med. Chem. Res.*, Vol. 21, pp. 681-693, 2012.
- [22] S. J. Cho and A. Tropsha, "Cross validated R2 guided region selection for comparative molecular field analysis: a simple method to achieve consistent results", *J. Med. Chem.*, Vol. 38, pp. 1060-1066, 1995.
- [23] S. Wold, M. Sjostrom, and L. Eriksson, "PLS regression: a basic tool of chemometrics", *Chemometr. Intell. Lab.*, Vol. 58, pp. 109-130, 2001.